





30 climate models (GCMs) can describe the response of the global circulation to large-scale forcing, such as  
31 greenhouse gases and solar radiation (Giorgi, 2019). But their horizontal resolutions are too coarse to account  
32 for the effects of local-scale forcing and processes, such as complex topography, land cover distribution, and  
33 dynamical processes occurring at the mesoscale (Giorgi et al., 2016; Qiu et al., 2017; Torma et al., 2015).  
34 Regional climate models (RCMs) have been applied to downscale the GCM outputs to finer scales in CA (Zhu  
35 et al., 2020; Ozturk et al., 2017; Mannig et al., 2013). However, their resolutions are still low ( $\geq 30$ km),  
36 especially for the mountainous areas in the southeast. Moreover, most of the previous RCM simulations used  
37 a single GCM as the lateral boundary conditions, which harbor high uncertainties in the projected climate  
38 changes.

39 The present authors carried out a study that involves the dynamical downscaling of multiple bias-  
40 corrected GCMs for the CA region with an unprecedented horizontal resolution of 9km. The future simulation  
41 period is set as 2031-2050 under Representative Concentration Pathway (RCP) 4.5, with the reference period  
42 of 1986-2005. The simulated surface air temperature and precipitation have been evaluated in a recent study  
43 (Qiu et al., 2021) and meanwhile basic features of the projected climate changes have been demonstrated. The  
44 results show that the high-resolution RCMs driven by bias-corrected GCMs are excellent in simulating the  
45 local temperature and precipitation in CA and detect significant warming, severer heatwaves, and drier  
46 conditions in this region in the near-term future.

47 To satisfy the urgent need of high-resolution climate data for ecological and hydrological applications in  
48 CA, the HCPD-CA (High-resolution Climate Projection Dataset in CA) dataset is derived from the 9-km  
49 resolution downscaled results, which includes ten meteorological elements (Table 1) that are widely used to  
50 drive ecological and hydrological models. They are daily precipitation (PREC, mm/day), daily  
51 mean/maximum/minimum temperature at 2m (T2MEAN/T2MAX/T2MIN, K), daily mean relative humidity  
52 at 2m (RH2MEAN, %), daily mean eastward and northward wind at 10m (U10MEAN/V10MEAN, m/s), daily  
53 mean downward shortwave/longwave flux at surface (SWD/LWD, W/m<sup>2</sup>), and daily mean surface pressure  
54 (PSFC, Pa). The present paper is to introduce this dataset to the community. Sect. 2 describes the regional  
55 model and experiments. Model evaluation and projected changes in these elements are in Sect. 3. Added values  
56 of using 9-km resolution respect to using coarser resolutions are discussed in Sect. 4 as well as uncertainties  
57 of the dataset. Sect. 5 describes access to the data product and all codes and tools. Main results are concluded  
58 in Sect. 6.



## 59 **2 Model and experiments**

### 60 **2.1 Regional model**

61 The Weather Research and Forecasting (WRF) model with version 3.8.1 (Skamarock et al., 2008) is used  
62 to downscale the GCMs. It has two domains (Fig. 1b). The outer one covers a large region, with a 27-km  
63 resolution and 290×205 grids. The inner one covers the CA region, with a 9-km resolution and 409×295 grids.  
64 The model has 33 levels in the vertical direction with its top fixed at 50 hPa. Its physical schemes are set based  
65 on our previous work about the sensitivity study of different physical parameterizations of the WRF model in  
66 simulating the local climate in CA (Wang et al., 2020). Details about them are in Qiu et al. (2021). Spectral  
67 nudging with a weak coefficient of  $3 \times 10^{-5}$  is applied in the outer domain (not in the inner one), which prevents  
68 possible model drift during the long-term integration by relaxing the model simulations of wind, temperature,  
69 and moisture toward the driving conditions. In addition to greenhouse gases and solar constant, the WRF  
70 model also considers other external forcing, such as aerosols, volcanoes, and ozone, to make its inner external  
71 forcing consistent with the driving GCMs.

### 72 **2.2 Bias-correction technique**

73 MPI-ESM-MR (referred to as MPI, Table 2), CCSM4 (referred to as CCSM), and HadGEM2-ES  
74 (referred to as Had) from Phase 5 of the Coupled Model Intercomparison Project (CMIP5) are selected to  
75 drive the regional model. Since all GCMs suffer from some forms of bias (Done et al., 2015; Ehret et al.,  
76 2012; Liang et al., 2008; Xu and Yang, 2012) that may propagate down to the RCM outputs, the bias-correction  
77 technique developed by Bruyère et al. (2014) is applied in this study to correct the climatology of the GCMs  
78 and allow synoptic and climate variability to change.

79 Six-hourly GCM data in a 25-year base/future period (1981-2005/2026-2050), hereafter referred to as  
80  $GCM_{BP}/GCM_{FP}$ , are broken down into the 25-year mean 6-hourly annual cycle over the base period ( $\overline{GCM_{BP}}$ )  
81 plus a 6-hourly perturbation term ( $GCM_{BP}'/GCM_{FP}'$ ):

$$82 \quad GCM_{BP} = \overline{GCM_{BP}} + GCM_{BP}' \quad (1)$$

$$83 \quad GCM_{FP} = \overline{GCM_{BP}} + GCM_{FP}' \quad (2)$$

84 The ERA-Interim reanalysis data (Dee et al., 2011, Table 2) as “observations” ( $Obs$ ) is similarly broken  
85 down into the mean annual cycle ( $\overline{Obs}$ ) and a perturbation term ( $Obs'$ ):

$$86 \quad Obs = \overline{Obs} + Obs' \quad (3)$$

87 The bias corrected GCM data for the base/future period,  $GCM_{BP}^*/GCM_{FP}^*$ , is then constructed by



88 replacing  $\overline{GCM_{BP}}$  from Eq. 1/2 with  $\overline{Obs}$  from Eq. 3:

89 
$$GCM_{BP}^* = \overline{Obs} + GCM_{BP}' \quad (4)$$

90 
$$GCM_{FP}^* = \overline{Obs} + GCM_{FP}' \quad (5)$$

91 Eq. 1-5 are applied to all the variables required to generate the initial and lateral boundary conditions for  
92 the WRF model: zonal and meridional wind, geopotential height, air temperature, relative humidity, sea  
93 surface temperature, mean sea level pressure, etc.

## 94 2.3 Experiments

95 The RCM simulations with the bias-corrected GCMs (MPI, CCSM, and Had) as the driving data are  
96 referred to as WRF\_MPI\_COR, WRF\_CCSM\_COR, and WRF\_Had\_COR, respectively (“COR” means using  
97 the bias-correction technique). The reference-period simulations are from December 1, 1985 to December 31,  
98 2005 and the future runs are from December 1, 2030 to the end of 2050 under a moderate carbon emission  
99 scenario RCP 4.5, which is arguably the most policy-relevant scenario as the Nationally Determined  
100 Contributions (NDCs) greenhouse gas emissions framework would produce similar temperatures trajectories  
101 (Gabriel and Kimon, 2015). The first month in each simulation is discarded as spin up. Fig. 2 shows the flow  
102 chart to produce the HCPD-CA dataset.

## 103 3 Results

### 104 3.1 Model evaluation

105 In Qiu et al. (2021), the key meteorological elements, surface air temperature and precipitation, have  
106 been evaluated with both gridded observations and stations’ data (see Sect. 3.1 in the paper) and the results  
107 show good skills of the regional model in simulating the local temperature and precipitation in CA during the  
108 reference period (1986-2005). Accordingly, the ten meteorological elements (including surface air temperature  
109 and precipitation) in the HCPD-CA dataset are evaluated here, to show the validity and applicability of the  
110 dataset. Note that daily mean wind speed at 10m (referred to as WS10MEAN) instead of U10MEAN and  
111 V10MEAN is evaluated.

112 Version 4 of the Climatic Research Units gridded Times Series (CRU TS v4, Harris et al., 2020, Table 2)  
113 is applied to evaluate T2MEAN/T2MAX/T2MIN and the fifth generation ECMWF (European Center for  
114 Medium Weather Forecasting) atmospheric reanalysis (ERA5, Hersbach et al., 2020, Table 2) land monthly  
115 averaged data (referred to as ERA-Land) is used as observations to evaluate other elements. Before the  
116 evaluation, the RCM outputs are interpolated to the grides of CRU TS v4 (ERA5-Land) with the distance-



117 weighted average (bilinear) method. We found that both on the annual and seasonal scales, the interpolation  
118 methods conserved the area averaged values in the model outputs with a bias of less than 1-2% between the  
119 original and new grids. We thus concluded that our choice of interpolation procedure does not affect the main  
120 conclusions of our work.

121 The high-resolution downscaled results (WRF\_MPI\_COR, WRF\_CCSM\_COR, and WRF\_Had\_COR)  
122 are very close to the observational data in simulating the climatology of all the elements in CA on the annual  
123 and seasonal scale (Fig. 3-5, seasonal results not shown here). For instance, the spatial correlation coefficients  
124 (SCCs) of all the elements except WS10MEAN are larger than 0.80. The SCCs of WS10MEAN are relatively  
125 small, in a range of 0.54-0.60. The regional model overestimated SWD, with the mean errors (MEs) in a range  
126 of 26.61-29.77 W/m<sup>2</sup>. Fig. 6 shows mean annual cycle of the monthly values averaged over CA. It is seen that  
127 the model outputs are generally close to the observations. The overestimation of SWD occurs throughout the  
128 year, with the bias larger in the warm seasons than in the cold seasons (Fig. 6e). The results of T2MAX and  
129 T2MIN are similar to those of T2MEAN (not shown here).

130 To sum up, the model evaluation shows the HCPD-CA dataset has good quality in describing the  
131 climatology of all the ten meteorological elements in CA, which ensures the suitability of the dataset for  
132 ecological and hydrological applications.

### 133 **3.2 Projected climate changes**

134 Fig. 7 shows projected changes of the annual mean values in CA during 2031-2050, relative to 1986-  
135 2005. All the RCM simulations exhibit significant warming over CA in the near-term future, with the annual  
136 mean T2MEAN increasing by 1.62-2.02°C (Fig. 7a-c). Pronounced warming is found in the north, which is  
137 attributed to the snow and surface albedo feedback (Qiu et al., 2021). Interestingly, enhanced warming  
138 projected in many mountains in the world (Palazzi et al., 2019; Pepin et al., 2015; Rangwala et al., 2013) is not  
139 found in CA (see Fig. 8 in Qiu et al. (2021)). It poses a question if the responses of ecological and hydrological  
140 systems to future warming in the Tien Shan and Pamirs differ from those in other mountains, like Tibetan  
141 Plateau/Himalayas and Alps.

142 The annual mean precipitation (PREC) is projected to slightly increase by 0.01-0.02 mm/day (Fig. 7d-f).  
143 However, changes in few areas passed the significance test. The annual mean RH2MEAN is projected to  
144 slightly decrease by 0.68-1.28% (Fig. 7g-i), which suggests a drier condition in CA in the coming decades and  
145 may affect the physical and chemical properties of the local vegetations. Changes in wind speed (WS10MEAN)  
146 are inconsistent among the RCM simulations (Fig. 7j-l). WRF\_MPI\_COR shows a slight increase of 0.02m/s  
147 while others show a slight decrease. Downward shortwave/longwave flux (SWD/LWD) are projected to



148 significantly increase by 3.47-4.28 W/m<sup>2</sup> and 7.13-9.61 W/m<sup>2</sup>, respectively (Fig. 7m-r). Surface pressure  
149 (PSFC) is simulated to slightly increase by 0.15-0.70 hPa in CA (Fig. 7s-u).

150 To sum up, the main feature of projected climate changes in CA in the near-term future is strong warming  
151 and significant increases in downward shortwave and longwave flux, with minor changes in other elements.  
152 Therefore, the HCPD-CA dataset provides extraordinary warming scenarios for assessing the impacts of future  
153 warming on the local ecological and hydrological systems in CA. Details about changes in these  
154 meteorological elements (e.g., changes at the seasonal scale) are out of the scope of the present paper and will  
155 be presented in further studies. Systematic analyses of changes in surface air temperature, heatwaves and  
156 droughts are in Qiu et al. (2021).

## 157 **4 Discussion**

### 158 **4.1 9km vs 27km**

159 As discussed above, most of the previous RCM simulations in CA have horizontal resolutions not higher  
160 than 30km. To show the added values of using 9-km resolution in this study respect to using coarser resolutions,  
161 the evaluation metrics (SCC and RMSE) of the simulated 9-km resolution precipitation in the inner domain  
162 of the WRF model are compared with those of 27-km resolution precipitation in the outer domain (Fig. 8). As  
163 the gridded observations (CRU TS v4, and ERA5-Land) have potential limitations in depicting the climatology  
164 of the elements in CA, the metrics are calculated based on 58 stations' data across CA (see red dots in Fig. 1a)  
165 which have been quality controlled (Qiu et al., 2021). Note that a station is compared with the model grid on  
166 which it is located.

167 Compared with the 27-km resolution data, the 9-km resolution data largely increases SCCs and reduces  
168 RMSEs, especially over the mountainous areas (see the subregion "MT" in Fig. 1c). For instance, over the  
169 mountainous areas, the ensemble-mean SCC of annual precipitation increases from 0.38 to 0.58 (Fig. 8c) and  
170 the ensemble-mean RMSE of annual precipitation decreases from 1.30 to 1.14 mm/day (Fig. 8d). This  
171 highlights the necessity of improving the model resolution from  $\geq 30$ km to 9km and the advantages of using  
172 the HCPD-CA dataset for researches in CA.

### 173 **4.2 Uncertainties**

174 With the limitation of the computational and time cost, this study used three bias-corrected GCMs from  
175 CMIP5 to do the dynamical downscaling over CA, which is an improvement relative to using a single original  
176 GCM. However, it still harbors uncertainties in the projected climate changes. As reported in the 1.5°C special



177 report of the Intergovernmental Panel on Climate Change (IPCC), we are on track to exceed 1.5°C warming  
178 between 2030 and 2052 based on the current warming rate, and hence the near-term future projection becomes  
179 more critical to human development than that for the end of this century. Therefore, this study focuses on  
180 climate changes over CA in the near-term future (2031-2050). Long-term continuous (e.g., 1986-2100)  
181 regional climate projections in CA are more useful for studies in this region and will be conducted in the next  
182 stage. Land-use and land-cover (LULC) in the WRF model is derived from the Moderate Resolution Imaging  
183 Spectroradiometer (MODIS) data of 2002 (Wang et al., 2007). Dramatic changes in water extent of the Aral  
184 Sea (Micklin, 2007) are not taken into account during the simulations, which brings uncertainties in simulating  
185 the local climate in this area as well as projecting the climate changes caused by changes in LULC.

## 186 **5. Data and code availability**

187 The HCPD-CA dataset is available at [http://data.tpdc.ac.cn/en/disallow/24c7467c-44a6-44ab-bbcf-](http://data.tpdc.ac.cn/en/disallow/24c7467c-44a6-44ab-bbcf-e6e346dd41d0/)  
188 [e6e346dd41d0/](http://data.tpdc.ac.cn/en/disallow/24c7467c-44a6-44ab-bbcf-e6e346dd41d0/) (Qiu, 2021). The files are stored in netCDF4 format and compiled using the Climate and  
189 Forecast (CF) conventions. It contains ten meteorological elements from three RCM simulations  
190 (WRF\_CCSSM\_COR, WRF\_MPI\_COR, and WRF\_Had\_COR) for a spatial domain covering the CA region  
191 (which is consisted of Kazakhstan, Kyrgyzstan, Tajikistan, Turkmenistan, and Uzbekistan) and its surrounding  
192 areas (see “D02” in Fig. 1b). The dataset covers two continuous 20-year periods, 1986-2005 and 2031-2050.  
193 Each year has 365 days (there is no leap year). We provide smaller-size (monthly and annual) files as  
194 surrogates for larger-size (daily) files. The names of the files follow the order: [dataset name]\_[experiment  
195 name]\_[element name]\_[year].[time frequency].nc. For example, the file name, HCPD-  
196 CA\_WRF\_CCSSM\_COR\_T2MAX\_2004.mon.nc, represents the monthly mean T2MAX of 2004 from the  
197 experiment WRF\_CCSSM\_COR in the HCPD-CA dataset.

198 The WRF model is available at [https://www2.mmm.ucar.edu/wrf/users/download/get\\_source.html](https://www2.mmm.ucar.edu/wrf/users/download/get_source.html). The  
199 source code to do the bias correction is available at <https://rda.ucar.edu/datasets/ds316.1/#!software>. The  
200 Climate Data Operators (CDO, <https://code.mpimet.mpg.de/projects/cdo>), Python modules (like netCDF4,  
201 Xarray, and Numpy), and NCAR Command Languages (NCL, <https://www.ncl.ucar.edu/>) are recommended  
202 to do operations on the netCDF files.

## 203 **6. Conclusions**

204 A high-resolution (9km) projection climate dataset in CA (the HCPD-CA dataset), containing ten  
205 meteorological elements, is derived from dynamically downscaled results based on three bias-corrected GCMs  
206 (MPI-ESM-MR, CCSM4, and HadGEM2-ES) from CMIP5 for ecological and hydrological applications in



207 this region. The reference and future periods are 1986-2005 and 2031-2050, respectively. The carbon emission  
208 scenario is RCP4.5. The model estimation shows good quality of the data product in describing the  
209 climatology of all the elements in CA, which ensures the suitability of the dataset. The RCM simulations  
210 commonly suggest strong warming over CA in the near-term future, with the annual mean T2MEAN  
211 increasing by 1.62-2.02°C, and significant increase in downward shortwave and longwave flux. Changes in  
212 other elements (e. g., precipitation, relative humidity at 2m, and wind speed at 10m) are minor. The HCPD-  
213 CA dataset presented here serves as a scientific basis for assessing the impacts of climate change over CA on  
214 many sectors, especially on ecological and hydrological systems.

## 215 **Author contribution**

216 All the authors made contributions to the conception or design of the work. YQ did the analyses and  
217 drafted the work and others revised it.

## 218 **Competing interests**

219 The authors declare that they have no conflict of interest

## 220 **Acknowledgements**

221 This study was supported by the Strategic Priority Research Program of Chinese Academy of Sciences  
222 (Grand No. XDA20020201) and the General Project of the National Natural Science Foundation of China  
223 (Grand No. 41875134). The work was carried out at National Supercomputer Center in Tianjin, and the  
224 calculations were performed on TianHe-1(A). The dataset is provided by National Tibetan Plateau Data Center  
225 (<http://data.tpsc.ac.cn>).

## 226 **References**

- 227 Bruyère, C. L., Done, J. M., Holland, G. J., and Fredrick, S.: Bias corrections of global models for regional  
228 climate simulations of high-impact weather, *Climate Dynamics*, 43, 1847-1856, 10.1007/s00382-013-  
229 2011-6, 2014.
- 230 Dee, D. P., Uppala, S. M., Simmons, A., Berrisford, P., Poli, P., Kobayashi, S., Andrae, U., Balmaseda, M.,  
231 Balsamo, G., and Bauer, d. P.: The ERA-Interim reanalysis: Configuration and performance of the data  
232 assimilation system, *Quarterly Journal of the royal meteorological society*, 137, 553-597, 2011.
- 233 Done, J. M., Holland, G. J., Bruyère, C. L., Leung, L. R., and Suzuki-Parker, A.: Modeling high-impact  
234 weather and climate: lessons from a tropical cyclone perspective, *Climatic Change*, 129, 381-395,  
235 10.1007/s10584-013-0954-6, 2015.
- 236 Ehret, U., Zehe, E., Wulfmeyer, V., Warrach-Sagi, K., and Liebert, J.: HESS Opinions "Should we apply bias  
237 correction to global and regional climate model data?", *Hydrol. Earth Syst. Sci.*, 16, 3391-3404,  
238 10.5194/hess-16-3391-2012, 2012.



- 239 Frenken, K.: Irrigation in Central Asia in figures, Food and Agriculture Organization of the United Nations,  
240 2013.
- 241 Gabriel, K. A., and Kimon, K.: Analysis of scenarios integrating the INDCs, EUR - Scientific and Technical  
242 Research Reports, 2015.
- 243 Gessner, U., Naeimi, V., Klein, I., Kuenzer, C., Klein, D., and Dech, S.: The relationship between precipitation  
244 anomalies and satellite-derived vegetation activity in Central Asia, *Global and Planetary Change*, 110,  
245 74-87, <https://doi.org/10.1016/j.gloplacha.2012.09.007>, 2013.
- 246 Giorgi, F., Torma, C., Coppola, E., Ban, N., Schär, C., and Somot, S.: Enhanced summer convective rainfall  
247 at Alpine high elevations in response to climate warming, *Nature Geoscience*, 9, 584-589,  
248 10.1038/ngeo2761, 2016.
- 249 Giorgi, F.: Thirty Years of Regional Climate Modeling: Where Are We and Where Are We Going next?,  
250 *Journal of Geophysical Research: Atmospheres*, 124, 5696-5723, 10.1029/2018jd030094, 2019.
- 251 Harris, I., Osborn, T. J., Jones, P., and Lister, D.: Version 4 of the CRU TS monthly high-resolution gridded  
252 multivariate climate dataset, *Scientific Data*, 7, 109, 10.1038/s41597-020-0453-3, 2020.
- 253 Hersbach, H., Bell, B., Berrisford, P., Hirahara, S., Horányi, A., Muñoz-Sabater, J., Nicolas, J., Peubey, C.,  
254 Radu, R., Schepers, D., Simmons, A., Soci, C., Abdalla, S., Abellan, X., Balsamo, G., Bechtold, P.,  
255 Biavati, G., Bidlot, J., Bonavita, M., De Chiara, G., Dahlgren, P., Dee, D., Diamantakis, M., Dragani, R.,  
256 Flemming, J., Forbes, R., Fuentes, M., Geer, A., Haimberger, L., Healy, S., Hogan, R. J., Hólm, E.,  
257 Janisková, M., Keeley, S., Laloyaux, P., Lopez, P., Lupu, C., Radnoti, G., de Rosnay, P., Rozum, I.,  
258 Vamborg, F., Villaume, S., and Thépaut, J.-N.: The ERA5 global reanalysis, *Quarterly Journal of the  
259 Royal Meteorological Society*, 146, 1999-2049, <https://doi.org/10.1002/qj.3803>, 2020.
- 260 Hong, S.-Y., Noh, Y., and Dudhia, J.: A New Vertical Diffusion Package with an Explicit Treatment of  
261 Entrainment Processes, *Monthly Weather Review*, 134, 2318-2341, 10.1175/MWR3199.1, 2006.
- 262 Iacono, M. J., Delamere, J. S., Mlawer, E. J., Shephard, M. W., Clough, S. A., and Collins, W. D.: Radiative  
263 forcing by long-lived greenhouse gases: Calculations with the AER radiative transfer models, *Journal of  
264 Geophysical Research: Atmospheres*, 113, 10.1029/2008JD009944, 2008.
- 265 Liang, X.-Z., Kunkel, K. E., Meehl, G. A., Jones, R. G., and Wang, J. X. L.: Regional climate models  
266 downscaling analysis of general circulation models present climate biases propagation into future change  
267 projections, *Geophysical Research Letters*, 35, <https://doi.org/10.1029/2007GL032849>, 2008.
- 268 Mannig, B., Müller, M., Starke, E., Merckenschlager, C., Mao, W., Zhi, X., Podzun, R., Jacob, D., and Paeth,  
269 H.: Dynamical downscaling of climate change in Central Asia, *Global and Planetary Change*, 110, 26-  
270 39, <https://doi.org/10.1016/j.gloplacha.2013.05.008>, 2013.
- 271 Micklin, P.: The Aral Sea disaster, in: *Annual Review of Earth and Planetary Sciences*, Annual Review of  
272 Earth and Planetary Sciences, 47-72, 2007.
- 273 Narama, C., Kääb, A., Duishonakunov, M., and Abdrakhmatov, K.: Spatial variability of recent glacier area  
274 changes in the Tien Shan Mountains, Central Asia, using Corona (~ 1970), Landsat (~ 2000), and ALOS  
275 (~ 2007) satellite data, *Global Planet Change*, 71, 42-54, 2010.
- 276 Niu, G.-Y., Yang, Z.-L., Mitchell, K. E., Chen, F., Ek, M. B., Barlage, M., Kumar, A., Manning, K., Niyogi,  
277 D., Rosero, E., Tewari, M., and Xia, Y.: The community Noah land surface model with  
278 multiparameterization options (Noah-MP): 1. Model description and evaluation with local-scale  
279 measurements, *Journal of Geophysical Research: Atmospheres*, 116, 10.1029/2010JD015139, 2011.
- 280 Ozturk, T., Turp, M. T., Türkeş, M., and Kurnaz, M. L.: Projected changes in temperature and precipitation  
281 climatology of Central Asia CORDEX Region 8 by using RegCM4.3.5, *Atmospheric Research*, 183, 296-  
282 307, <https://doi.org/10.1016/j.atmosres.2016.09.008>, 2017.
- 283 Palazzi, E., Mortarini, L., Terzago, S., and von Hardenberg, J.: Elevation-dependent warming in global climate  
284 model simulations at high spatial resolution, *Climate Dynamics*, 52, 2685-2702, 10.1007/s00382-018-  
285 4287-z, 2019.



- 286 Pepin, N., Bradley, R. S., Diaz, H. F., Baraer, M., Caceres, E. B., Forsythe, N., Fowler, H., Greenwood, G.,  
287 Hashmi, M. Z., Liu, X. D., Miller, J. R., Ning, L., Ohmura, A., Palazzi, E., Rangwala, I., Schöner, W.,  
288 Severskiy, I., Shahgedanova, M., Wang, M. B., Williamson, S. N., Yang, D. Q., and Mountain Research  
289 Initiative, E. D. W. W. G.: Elevation-dependent warming in mountain regions of the world, *Nature*  
290 *Climate Change*, 5, 424-430, 10.1038/nclimate2563, 2015.
- 291 Qiu, Y., Hu, Q., and Zhang, C.: WRF simulation and downscaling of local climate in Central Asia,  
292 *International Journal of Climatology*, 37, 513-528, 10.1002/joc.5018, 2017.
- 293 Qiu, Y., Feng, J., Yan, Z., Wang, J., and Li, Z.: High-resolution dynamical downscaling for regional climate  
294 projection in Central Asia based on bias-corrected multiple GCMs, *Climate Dynamics*, 10.1007/s00382-  
295 021-05934-2, 2021.
- 296 Rangwala, I., Sinsky, E., and Miller, J. R.: Amplified warming projections for high altitude regions of the  
297 northern hemisphere mid-latitudes from CMIP5 models, *Environmental Research Letters*, 8, 024040,  
298 10.1088/1748-9326/8/2/024040, 2013.
- 299 Seddon, A. W., Macias-Fauria, M., Long, P. R., Benz, D., and Willis, K. J.: Sensitivity of global terrestrial  
300 ecosystems to climate variability, *Nature*, 531, 229-232, 2016.
- 301 Skamarock, W. C., Klemp, J. B., Dudhia, J., Gill, D. O., Barker, D. M., Wang, W., and Powers, J. G.: A  
302 description of the Advanced Research WRF version 3. NCAR Technical note-475+ STR, 2008.
- 303 Sorg, A., Bolch, T., Stoffel, M., Solomina, O., and Beniston, M.: Climate change impacts on glaciers and  
304 runoff in Tien Shan (Central Asia), *Nature Climate Change*, 2, 725-731, 10.1038/nclimate1592, 2012.
- 305 Thompson, G., and Eidhammer, T.: A Study of Aerosol Impacts on Clouds and Precipitation Development in  
306 a Large Winter Cyclone, *Journal of the Atmospheric Sciences*, 71, 3636-3658, 10.1175/jas-d-13-0305.1,  
307 2014.
- 308 Torma, C., Giorgi, F., and Coppola, E.: Added value of regional climate modeling over areas characterized by  
309 complex terrain—Precipitation over the Alps, *Journal of Geophysical Research: Atmospheres*, 120,  
310 3957-3972, 10.1002/2014JD022781, 2015.
- 311 Wang, W., Barker, D., Bray, J., Bruyere, C., Duda, M., Dudhia, J., Gill, D., Michalakes, J. J. M., and Research,  
312 M. M. D. N. C. f. A.: User's guide for advanced research WRF (ARW) modeling system version 3, 2007.
- 313 Wang, Y., Feng, J., Luo, M., Wang, J., and Qiu, Y.: Uncertainties in simulating central Asia: Sensitivity to  
314 physical parameterizations using Weather Research and Forecasting model, *International Journal of*  
315 *Climatology*, 40, 5813-5828, <https://doi.org/10.1002/joc.6567>, 2020.
- 316 Xu, Z., and Yang, Z.-L.: An Improved Dynamical Downscaling Method with GCM Bias Corrections and Its  
317 Validation with 30 Years of Climate Simulations, *Journal of Climate*, 25, 6271-6286, 10.1175/JCLI-D-  
318 12-00005.1, 2012.
- 319 Zhang, C., Wang, Y., and Hamilton, K.: Improved Representation of Boundary Layer Clouds over the  
320 Southeast Pacific in ARW-WRF Using a Modified Tiedtke Cumulus Parameterization Scheme, *Monthly*  
321 *Weather Review*, 139, 3489-3513, 10.1175/mwr-d-10-05091.1, 2011.
- 322 Zhang, C., Lu, D., Chen, X., Zhang, Y., Maisupova, B., and Tao, Y.: The spatiotemporal patterns of vegetation  
323 coverage and biomass of the temperate deserts in Central Asia and their relationships with climate  
324 controls, *Remote Sens Environ*, 175, 271-281, 10.1016/j.rse.2016.01.002, 2016.
- 325 Zhu, X., Wei, Z., Dong, W., Ji, Z., Wen, X., Zheng, Z., Yan, D., and Chen, D.: Dynamical downscaling  
326 simulation and projection for mean and extreme temperature and precipitation over central Asia, *Climate*  
327 *Dynamics*, 10.1007/s00382-020-05170-0, 2020.
- 328
- 329



330 **Tables and Figures**

331 **Table 1** Meteorological elements in the HCPD-CA dataset

Element name	Description	Unit
PREC	Daily precipitation	mm/day
T2MEAN	Daily mean temperature at 2m	K
T2MAX	Daily maximum temperature at 2m	K
T2MIN	Daily minimum temperature at 2m	K
RH2MEAN	Daily mean relative humidity at 2m	%
U10MEAN	Daily mean eastward wind at 10m	m/s
V10MEAN	Daily mean northward wind at 10m	m/s
SWD	Daily mean downward shortwave flux at surface	W/m <sup>2</sup>
LWD	Daily mean downward longwave flux at surface	W/m <sup>2</sup>
PSFC	Daily mean surface pressure	Pa

332

333



334

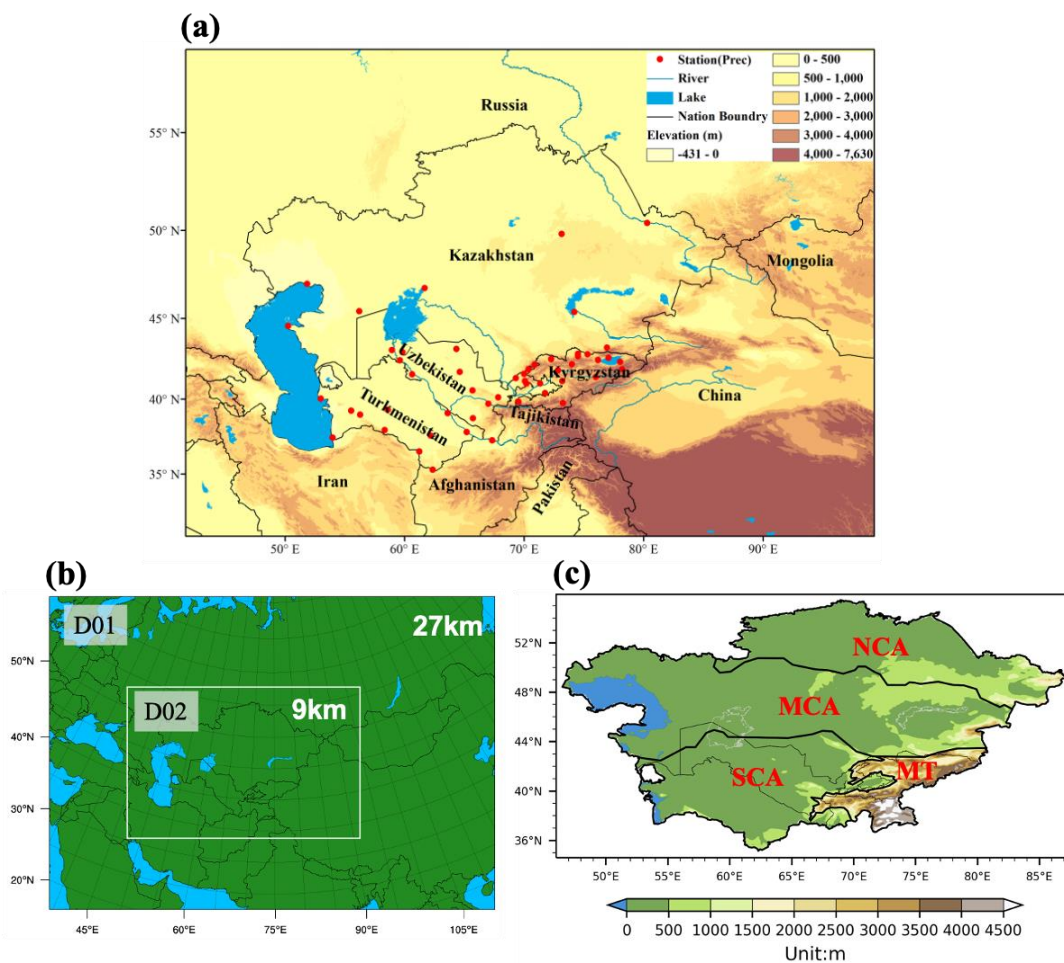
335

**Table 2** Information about the datasets used in the study.

<b>Dataset</b>	<b>Run</b>	<b>Spatial Resolution</b>	<b>Temporal Resolution</b>	<b>Link</b>
<b>MPI-ESM-MR</b>	ri11p1	1.9°×1.9°	6-hourly	<a href="https://esgf-node.llnl.gov/projects/cmip5/">https://esgf- node.llnl.gov/projects/cmip5/</a>
<b>HadGEM2-ES</b>	ri11p1	1.3°×1.9°	6-hourly	<a href="https://esgf-node.llnl.gov/projects/cmip5/">https://esgf- node.llnl.gov/projects/cmip5/</a>
<b>CCSM4</b>	b40.[20th\RCP 4.5].track1.1de g.012.cam2.h4	0.9°×1.3°	6-hourly	<a href="https://rda.ucar.edu/datasets/ds316.0/#!access">https://rda.ucar.edu/datasets/ ds316.0/#!access</a>
<b>ERA-Interim</b>	-	0.75°×0.75°	Synoptic monthly means	<a href="https://apps.ecmwf.int/dataset/data/interim-full-mnth/levtype=sfc/">https://apps.ecmwf.int/dataset/ data/interim-full- mnth/levtype=sfc/</a>
<b>CRU TS v4</b>	-	0.5°×0.5°	monthly	<a href="https://crudata.uea.ac.uk/cru/data/hrg/cru_ts_4.00/">https://crudata.uea.ac.uk/cru/ data/hrg/cru_ts_4.00/</a>
<b>ERA5-Land</b>	-	0.1°×0.1°	monthly	<a href="https://cds.climate.copernicus.eu/cdsapp#!/dataset/reanalysis-era5-land-monthly-means?tab=form">https://cds.climate.copernicu s.eu/cdsapp#!/dataset/reanaly sis-era5-land-monthly- means?tab=form</a>

336

337

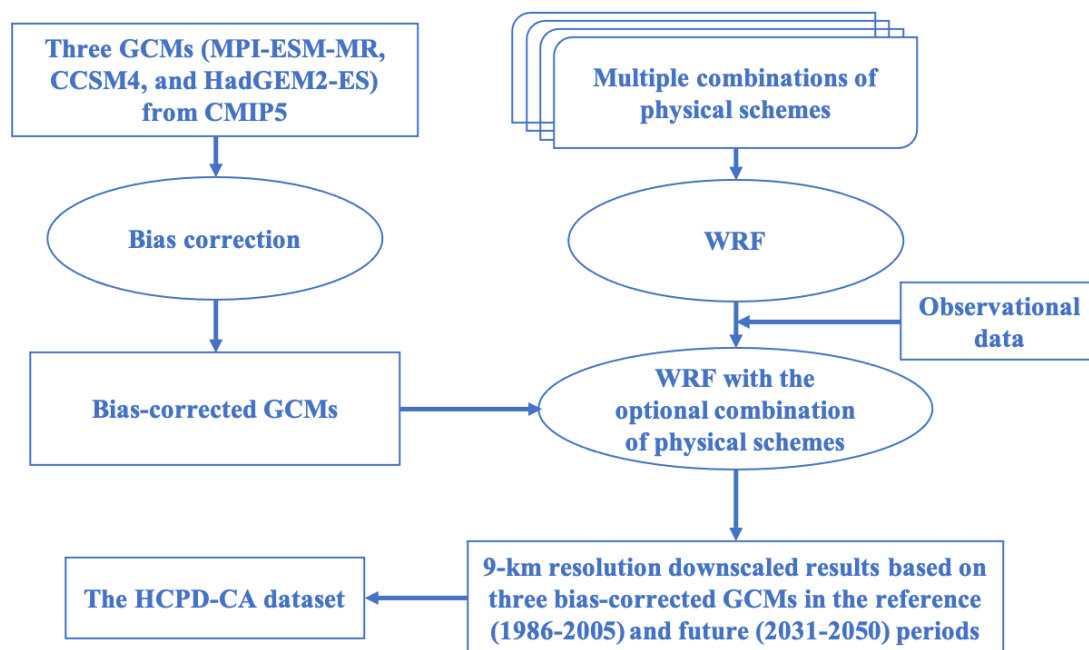


338

339 **Fig. 1** Central Asia (referred to as CA) and its surrounding (a), nested domains in the WRF model (b), and  
 340 climate subregions in CA (c). In subplot a, stations with records of precipitation are marked by red dots. In  
 341 subplot c, according to Qiu et al. (2021), the CA region is divided into four climate sub-regions: northern CA  
 342 (NCA), middle CA (MCA), southern CA (SCA), and the mountainous areas (MT). This figure is adapted from  
 343 Qiu et al. (2021) and the reproduction right has been granted.  
 344

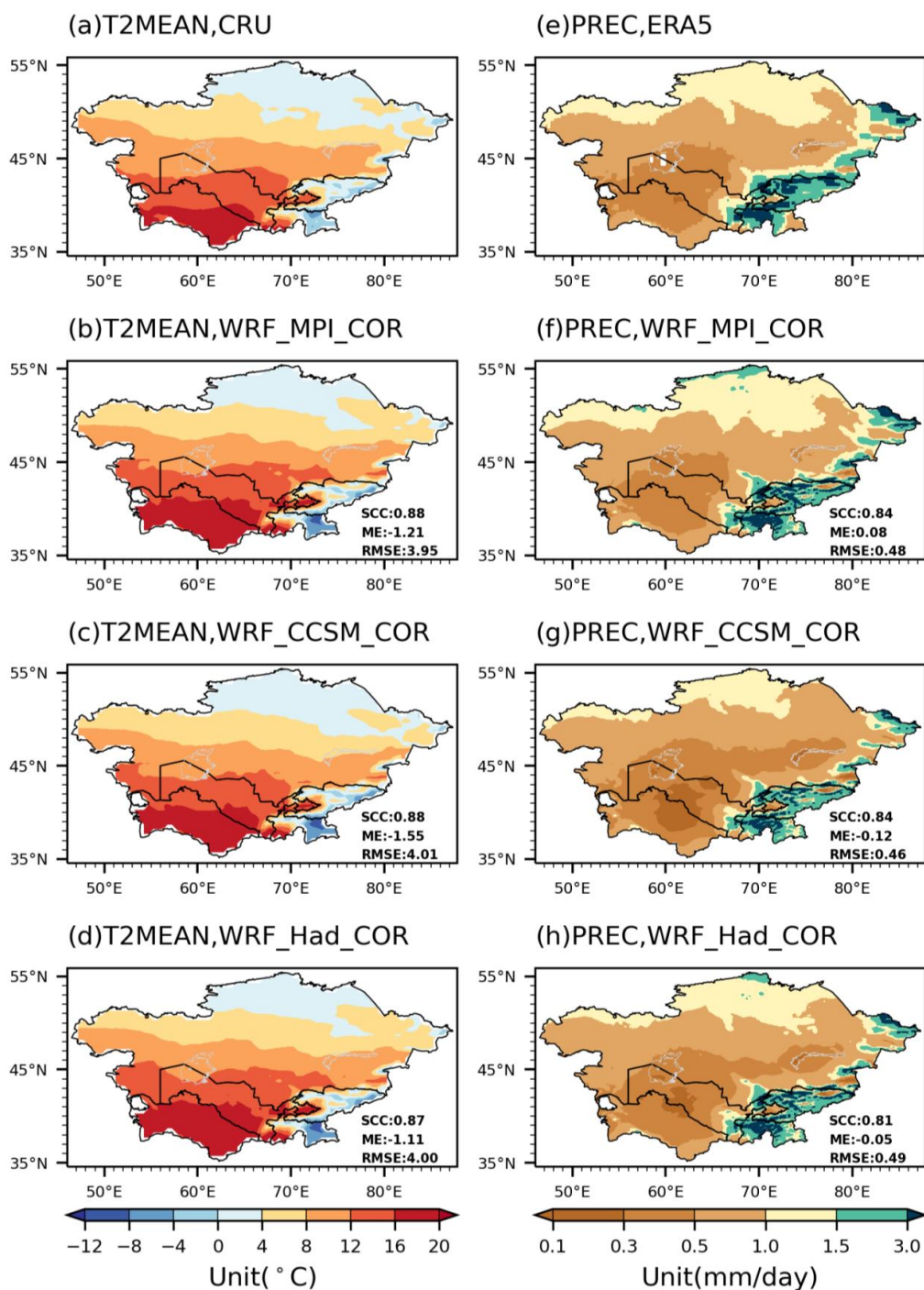


345



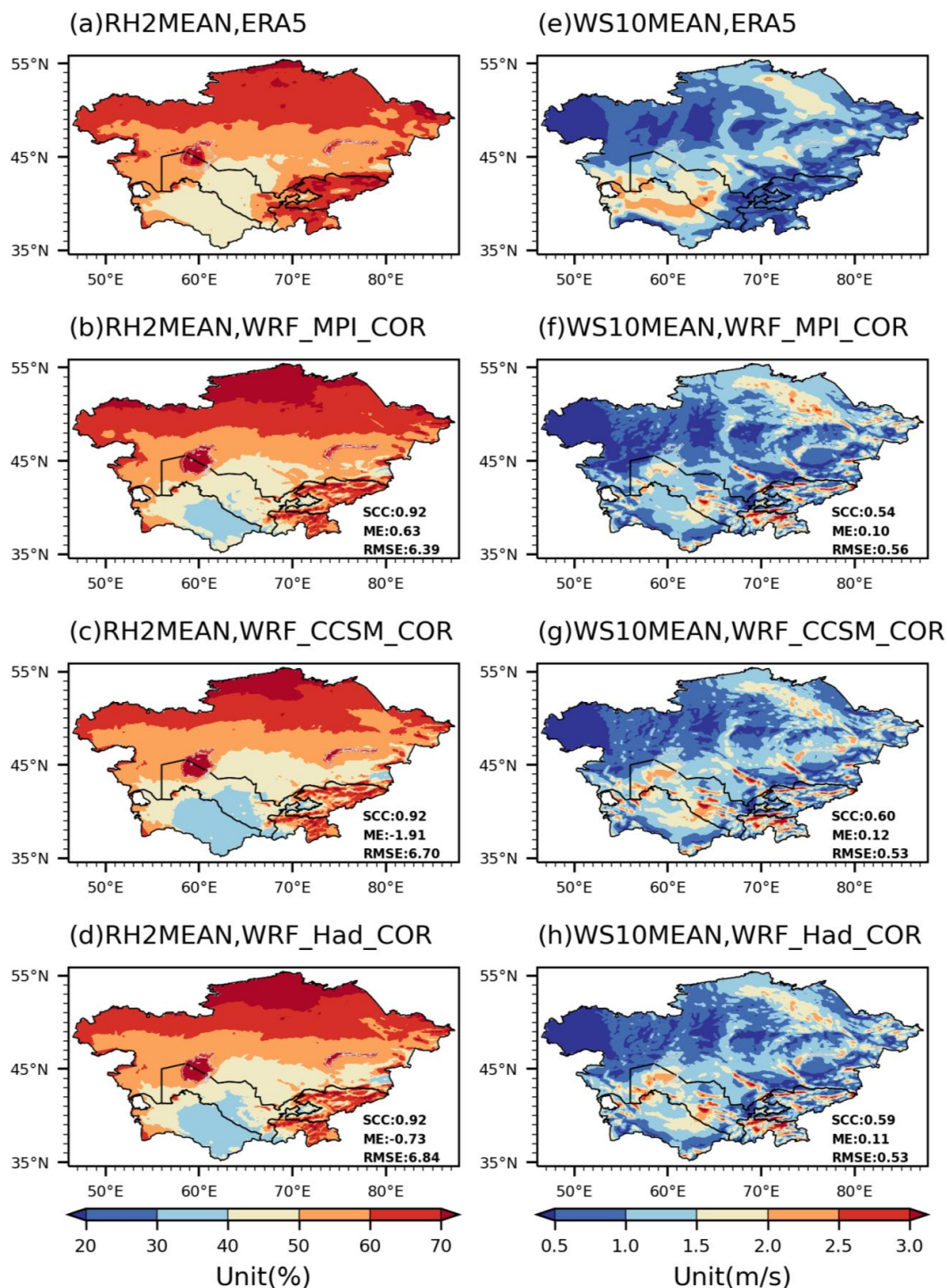
346

347 **Fig. 2** Flow chart for the HCPD-CA dataset.



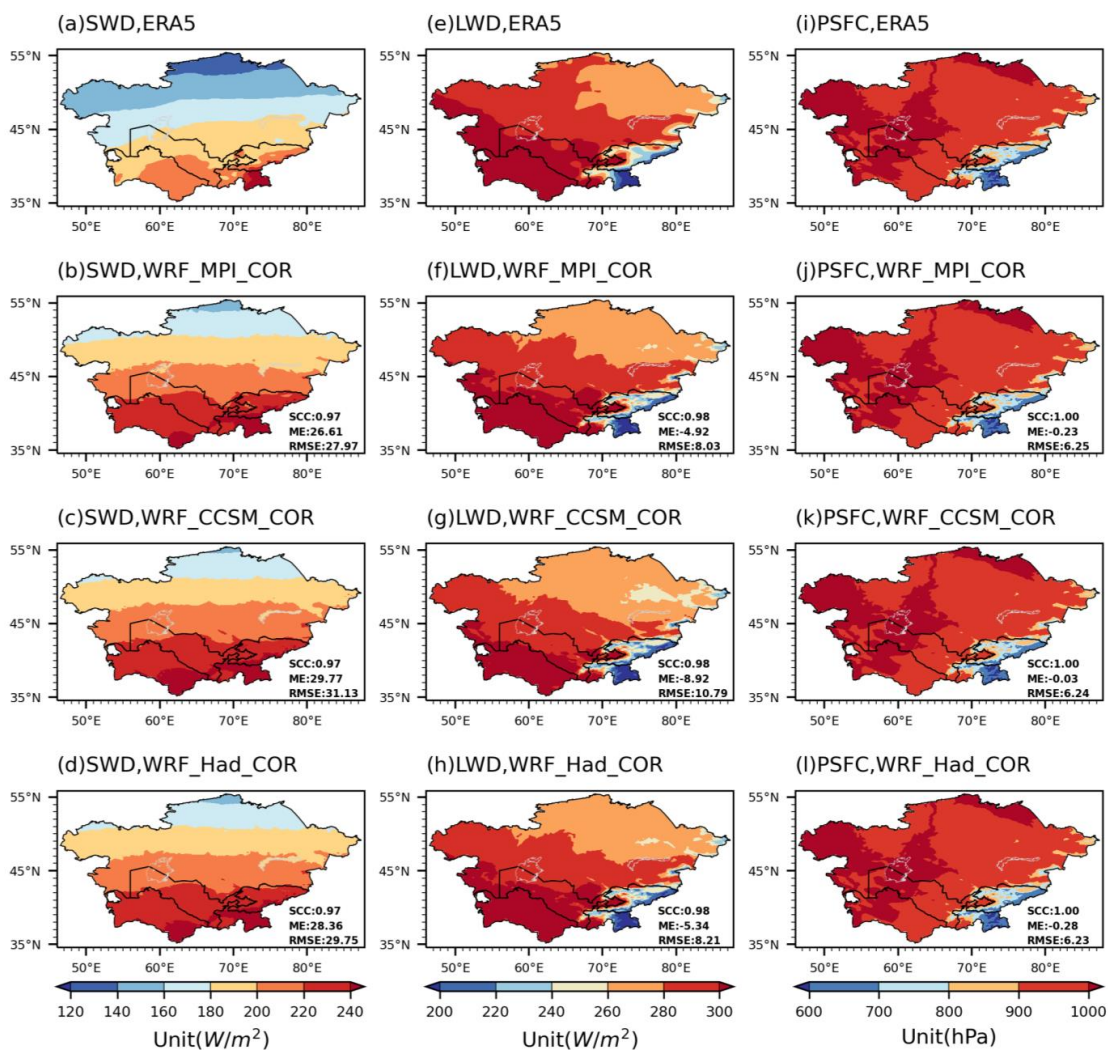
348

349 **Fig. 3** The observed and simulated annual mean T2MEAN and PREC in Central Asia during the reference  
 350 period (1986-2005). The spatial correlation coefficient (SCC), mean error (ME), and root mean square error  
 351 (RMSE) are listed.



352

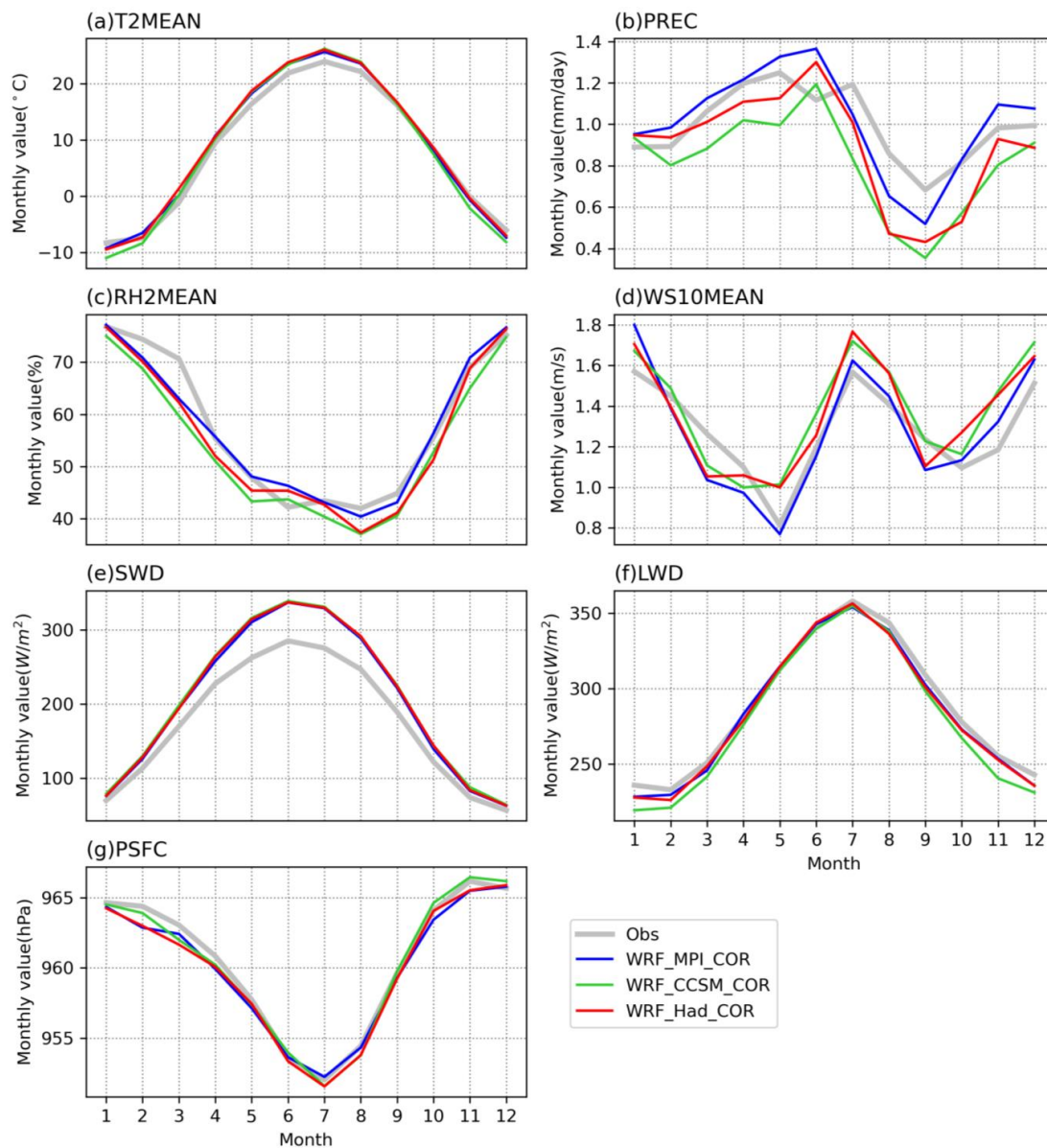
353 **Fig. 4** Same as **Fig. 3**, but for annual mean RH2MEAN and WS10MEAN.



354

355 **Fig. 5** Same as **Fig. 3**, but for annual mean SWD, LWD, and PSFC.

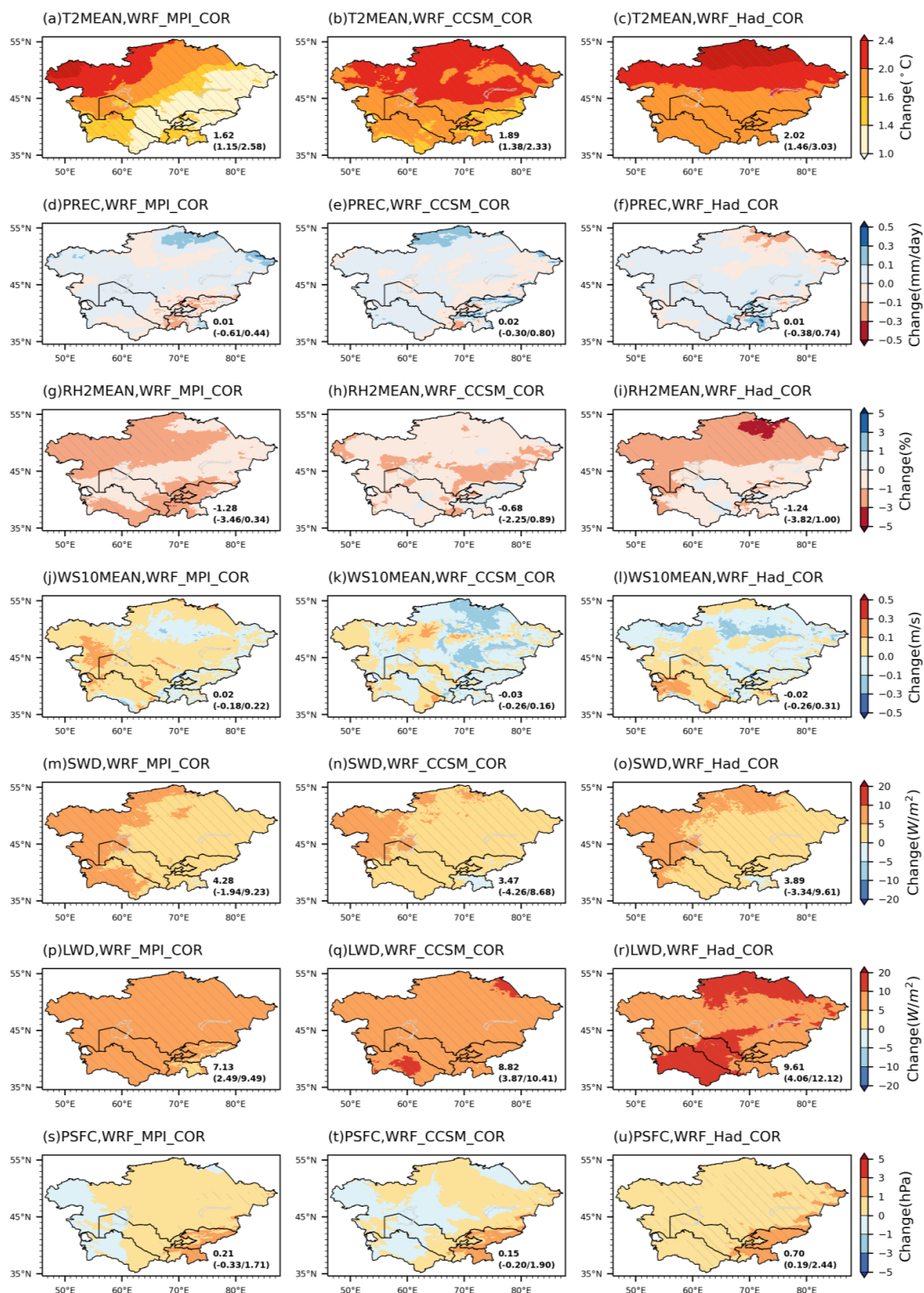
356



357

358 **Fig. 6** Mean annual cycle of the monthly values averaged over Central Asia in the observation and RCM  
359 simulations.

360

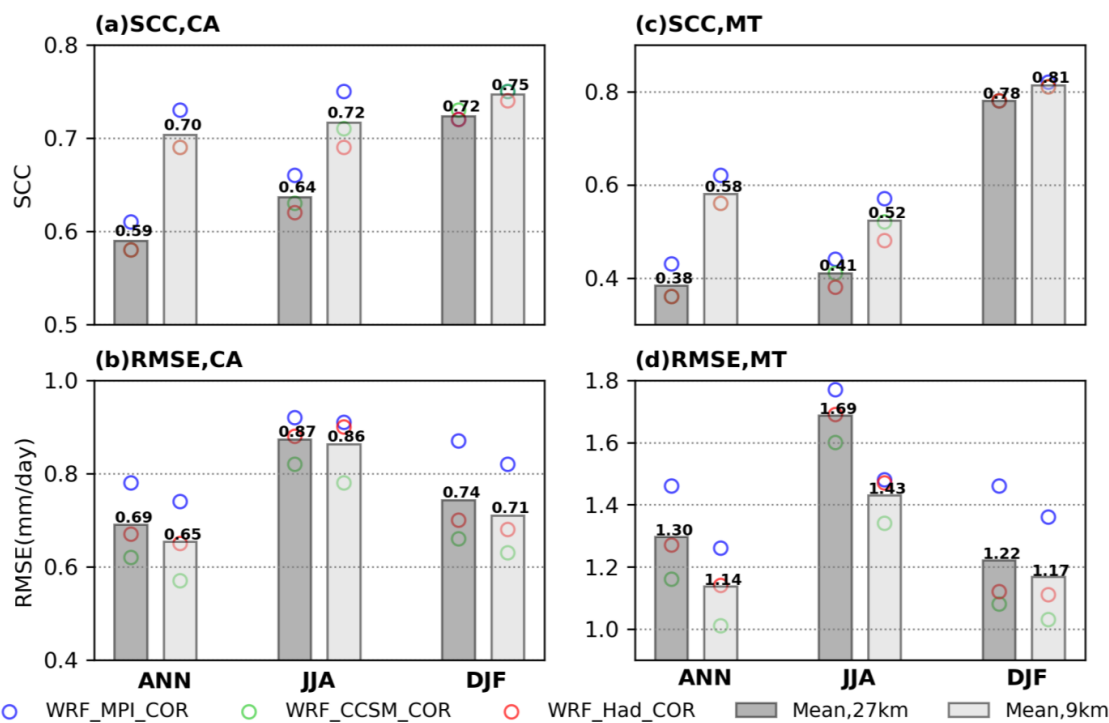


361

362 **Fig. 7** Projected changes of the annual mean values over Central Asia during 2031-2050, relative to 1986-



363 2005. The regional mean (upper), minimum and maximum value (in parentheses) are listed. The slashed areas  
 364 indicate where the changes passed the significance test at the 95% confidence level using the two-tailed  
 365 Student's t test.  
 366



367 ○ WRF\_MPI\_COR ○ WRF\_CCSM\_COR ○ WRF\_Had\_COR ■ Mean,27km ■ Mean,9km  
 368 **Fig. 8** Spatial correlation coefficients (SCCs) and root mean square errors (RMSEs) of the simulated annual  
 369 (ANN), summer (JJA: June-July-August), and winter (DJF: December-January-February) mean precipitation  
 370 over CA and the mountainous areas (MT) in the 9-km and 27-km resolution downscaled results. The metrics  
 371 are calculated based on 58 stations' data across CA.

372  
 373